

# Application of Rayleigh waves on PS-wave static corrections

Chunying Yang<sup>1</sup>, Yun Wang<sup>2,4</sup> and Jun Lu<sup>3</sup>

<sup>1</sup> Institute of Geology & Geophysics, Chinese Academy of Sciences, Beijing 100029, People's Republic of China

<sup>2</sup> Institute of Geochemistry, Chinese Academy of Sciences, Guiyang 550002, People's Republic of China

<sup>3</sup> Key Laboratory of Marine Reservoir Evolution and Hydrocarbon Accumulation Mechanism, Ministry of Education of China, China University of Geosciences, Beijing 100083, People's Republic of China

E-mail: [yangchunying07@mail.gucas.ac.cn](mailto:yangchunying07@mail.gucas.ac.cn), [yunwang@mail.iggcas.ac.cn](mailto:yunwang@mail.iggcas.ac.cn) and [lujun@mail.iggcas.ac.cn](mailto:lujun@mail.iggcas.ac.cn)

Received 22 December 2010

Accepted for publication 18 November 2011

Published 22 December 2011

Online at [stacks.iop.org/JGE/9/90](http://stacks.iop.org/JGE/9/90)

## Abstract

Due to lack of information about near-surface S-wave velocities, especially in the areas where near-surface structure and the subsurface are complex, receiver static corrections become one of the key steps in multi-component converted PS-wave data processing. In this paper, we first extract Rayleigh waves from the field shot records and obtain near-surface S-wave velocities based on the inversion of Rayleigh wave dispersion curves. The receiver statics of PS-waves are then calculated via P-wave statics. Finally, the method introduced in this paper is applied in 2D/3D seismic field data processing, which shows that S-wave statics are larger than P-wave statics and vary dramatically in the horizon directions; the PS-wave stack sections are improved after applying PS-wave statics. It can be concluded that this method is feasible for PS-wave static corrections.

**Keywords:** PS-wave, static correction, Rayleigh wave, dispersion, S-velocity

## 1. Introduction

Time delays due to PS-waves travelling through the weathered layer make the routine static correction procedure unsuitable for PS-wave static corrections in multi-component data processing. Considering rays travelling in the subsurface, PS-wave static correction includes P-wave static corrections for shot points and S-wave static corrections for receivers (Cox 1999). Shot statics can be calculated using conventional seismic processing methods (Chang *et al* 2002, Ronen and Claerbout 1985, Vasudevan *et al* 1991), while receiver statics are difficult to calculate in seismic data processing due to lack of near-surface S-wave velocities. Also, the statics for S-waves are larger than those of P-waves since S-wave velocities are lower than P-wave velocities (Lawton 1989, Tatham *et al* 1991).

Some methods for PS-wave static corrections have been developed, i.e. residual static corrections for P-waves, which are based on statistical analysis and avoid computing S-wave

statics of receivers based on an S-wave velocity model (Cary and Eaton 1993, Normark 1993, Wang *et al* 1997). However, those methods cannot give an accurate calculation of PS-wave statics when near-surface S-wave velocities vary dramatically in vertical and horizontal directions. Furthermore, the large statics for S-waves cannot be handled by residual static corrections when S-wave velocities in the weathered layer are 20%–50% lower than P-wave velocities (Kano *et al* 2003).

Until now, much effort has been made in deriving near-surface S-wave velocities. Dix (1955) introduced an S-wave inversion method based on shear wave logging, reflection and refraction analysis. Schafer (1989, 1991), Meulenbroek (2011) and Hearn (2011) employed shear wave refractions to obtain near-surface S-wave velocities. Yao (1991) developed a method to improve first arrival pickings of shear waves through the  $\tau$ -p transform. Li *et al* (1990) put forward a topographic method to obtain S-wave velocities. Zhao *et al* (1992) applied this method to construct the subsurface S-wave velocity models according to earthquake signals from northeastern Japan.

<sup>4</sup> Author to whom any correspondence should be addressed.

However the above methods are no longer feasible when S-wave first arrivals are seriously contaminated with those of P-waves (Palmer 1986). Xia *et al* (1999) introduced a method to calculate S-wave velocities through the inversion of Rayleigh wave dispersion curves. In the area where surface waves are strong and first arrivals of shear waves cannot be identified and picked up, this method can provide a relatively accurate S-wave velocity model.

It has been discussed that Rayleigh waves can be applied to invert near-surface S-wave velocities according to the relation between Rayleigh and body waves (Sheriff and Geldart 1982, Sheriff 1991, Yang 1993). In petroleum seismic exploration, Rayleigh waves become a kind of ‘useful wave’ when Rayleigh waves are used to calculate PS-wave statics. In this paper, we use Rayleigh waves to invert the near-surface S-wave velocities and then calculate receiver statics rather than deriving S-wave velocity models through field surveys.

## 2. Fundamental method

### 2.1. Theoretical background

Rayleigh waves travel along a free surface with retrograde and elliptical particle motions. The amplitude of Rayleigh waves decays inversely proportional to the square root of the distance from the source, while the amplitude of body waves, such as P- or S-waves, decreases inversely proportional to the distance from the source (Sheriff and Geldart 1995). In addition, Rayleigh waves with different frequencies propagate with different velocities in layered media, i.e. Rayleigh waves are dispersive. The frequency equation for Rayleigh waves in an elastic half-space (Graff 1975) is

$$r^3 - 8r^2 + \left(24 - 16 \left(\frac{V_S}{V_P}\right)^2\right)r + 16 \left(\left(\frac{V_S}{V_P}\right)^2 - 1\right) = 0, \quad (1)$$

where  $r = (V_R/V_S)^2$ ;  $V_R$  and  $V_S$  are the phase velocities of Rayleigh and S-waves, respectively. Poisson’s ratio  $\sigma$  is defined as (Grant and West 1965)

$$\sigma = (V_P^2 - 2V_S^2)/[2(V_P^2 - V_S^2)], \quad (2)$$

where  $V_P$  is the P-wave velocity. The S-wave velocity  $V_S$  can be estimated using equation (3) based on the Rayleigh wave velocity  $V_R$  and Poisson’s ratio  $\sigma$  (Potel and de Belleval 1995):

$$V_S = \left(\frac{0.87 + 1.12\sigma}{1 + \sigma}\right)^{-1} V_R. \quad (3)$$

In a special case, it can be approximated that the S-wave velocity  $V_S \approx \frac{V_R}{0.92}$ , when  $\sigma = 0.25$ .

The characteristic equation of the Rayleigh wave phase velocity (Schwab and Knopoff 1970) is given by

$$F(w, V_{Rm}, V_{Pm}, V_{Sm}, \rho_m, h_m) = 0, \quad m = 1, \dots, N, \quad (4)$$

where  $w$  is frequency,  $V_{Pm}$ ,  $V_{Sm}$ ,  $\rho_m$  and  $h_m$  are P- and S-wave velocities, densities and thicknesses of layers, respectively. For the layered media, Rayleigh wave phase velocities can be calculated by Knopoff’s method. Because Rayleigh wave dispersion curves are more sensitive to S-wave velocities and thicknesses rather than densities and P-wave velocities

(Xia *et al* 1999), we use Rayleigh wave dispersion curves to invert the near-surface S-wave velocities and thicknesses; other parameters are assumed as *a priori* information in the inversion process.

According to equation (4), we define an objective function

$$J = \sqrt{\sum_{n=1}^N (V_{\text{mod } n} - V_{\text{obs } n})^2 / N}, \quad (5)$$

where  $V_{\text{mod } n}$  is the Rayleigh wave phase velocity responding to the initial near-surface model;  $V_{\text{obs } n}$  is the observed Rayleigh wave phase velocity; and  $N$  is the number of observed frequency–velocity couples.

By minimizing the objective function using a genetic algorithm (Houck *et al* 1995), we will derive a solution of the S-wave velocity model. This method can avoid suboptimal solutions because it can explore the solution in multiple directions. The population in the genetic algorithm consists of several initial models, and each of them is an individual of the population. The fittest individuals are iterative solutions of the inversion procedure. Based on the genetic algorithm, a set of initial model parameters ( $V_{Pi}$ ,  $V_{Si}$ ,  $\rho_i$  and  $h_i$ ) should be given before inversion processes. These are defined as follows:

$$V_S = \{V_{S1 \min} \leq V_{S1} \leq V_{S1 \max}, V_{S2 \min} \leq V_{S2} \leq V_{S2 \max}, \dots\}, \quad (6)$$

$$h = \{h_{1 \min} \leq h_1 \leq h_{1 \max}, h_{2 \min} \leq h_2 \leq h_{2 \max}, \dots\}, \quad (7)$$

where  $V_{Si \min}$  and  $V_{Si \max}$  are the minimum and the maximum S-wave velocity of the  $i$ th layer; and  $h_{i \min}$  and  $h_{i \max}$  are the minimum and the maximum thickness of the  $i$ th layer.  $V_{Pi}$  and  $\rho_i$  are *a priori* information.

Equation (4) is then used to calculate Rayleigh wave phase velocities of the initial models. The solution of minimizing the objective function (5) is the inverted S-wave velocity model. To obtain a better inversion result, we should make a good choice of parameters such as the fitness function and the size of the population in the inversion algorithm.

Before inversion, we must extract Rayleigh wave dispersion curves. Various methods used to attenuate surface waves can be applied to extract Rayleigh wave dispersion curves, such as  $f$ – $k$  (frequency–wavenumber) domain filtering slowness-frequency method (Benhama *et al* 1988, Park *et al* 1999). Park *et al* (1998) construct high-resolution images of dispersion curves by the wavefield transformation method. This method is applied to calculate dispersion curves of Rayleigh waves for the inversion process. A synthetic shot gather and the dispersion relation are displayed in figures 1(a) and (b), respectively. Figure 1(c) shows the image of dispersion curve obtained by applying this method to figure 1(a).

Then, S-wave velocities can be inverted with equation (5). The receiver statics of the S-waves are calculated using the near-surface S-wave velocities. Procedures for estimation of PS-wave statics are similar to P-wave processing, as outlined below.

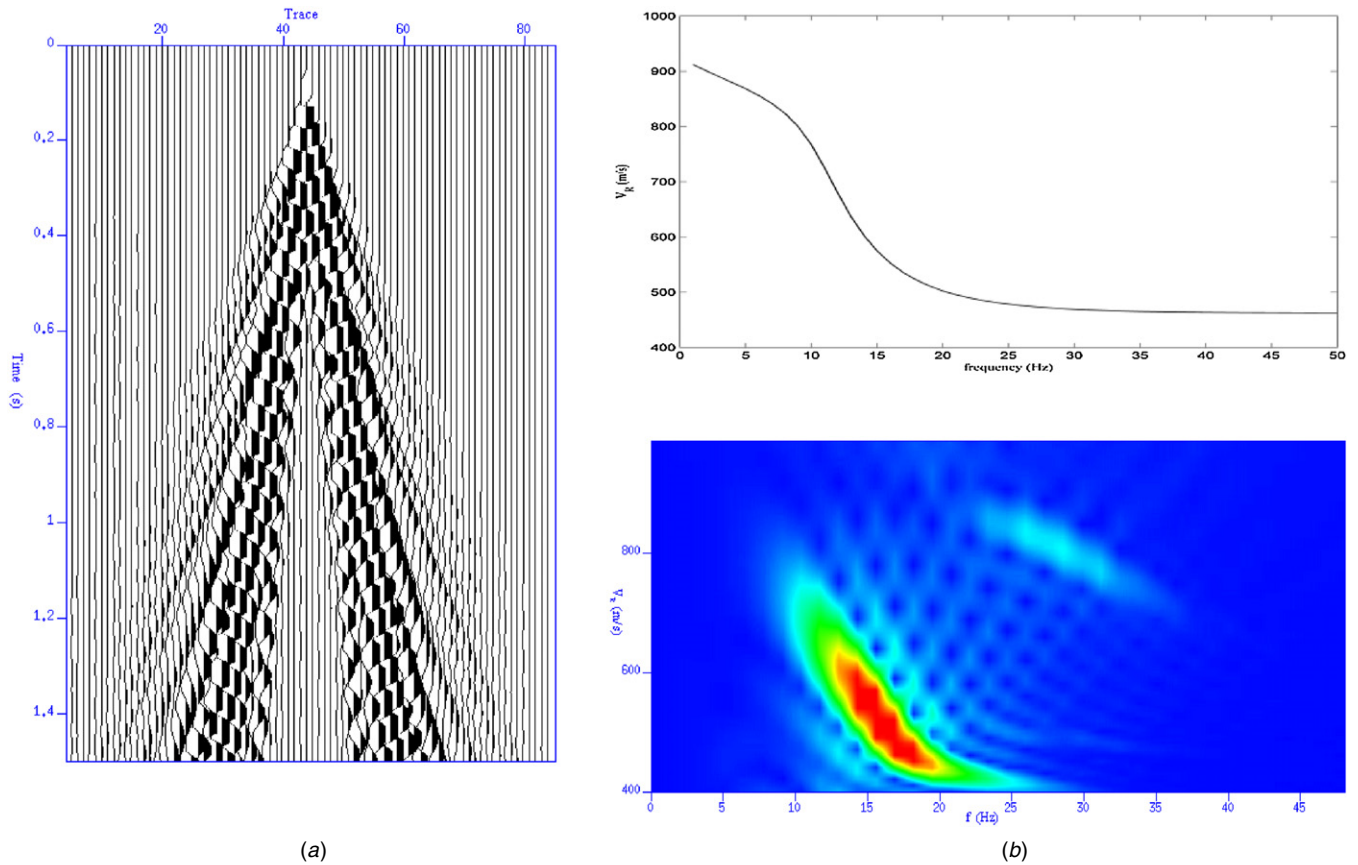


**Figure 1.** (a) A synthetic shot gather, (b) dispersion relation and (c) image of the dispersion curve of the synthetic data.

## 2.2. Processing procedures

First, we start with extracting Rayleigh waves from shot records; afterwards, higher signal-to-noise ratio (SNR) Rayleigh wave records are selected. Second, we pick up frequency–velocity couples using the wavefield transformation method. Third, we construct a near-surface S-wave velocity model with the genetic algorithm, based on Rayleigh wave dispersion curves. It is an iterative process and initial models are needed, in which S-wave velocities, thicknesses and the number of layers must be included. Next, we select a seismic datum to calculate static corrections. The datum for S-wave static corrections should be consistent with that for P-wave (Yao 1991). The procedure of selecting a seismic datum for static corrections will be easier if micro-logging or a refraction survey can provide more information about the near-surface S-wave velocities (Wiest and Edelmann 2006). Finally, we estimate the receiver statics according to the inverted S-wave model. The process workflow of building the near-surface S-wave velocity model is shown in figure 2.

Two important notes should be emphasized. S-wave velocities need to be inverted in iterations according to subsurface geological models. When a consistent interface for S- and P-wave velocities cannot be found, the statics for S-waves can be calculated according to P-wave statics and P- to S-wave velocity ratio.

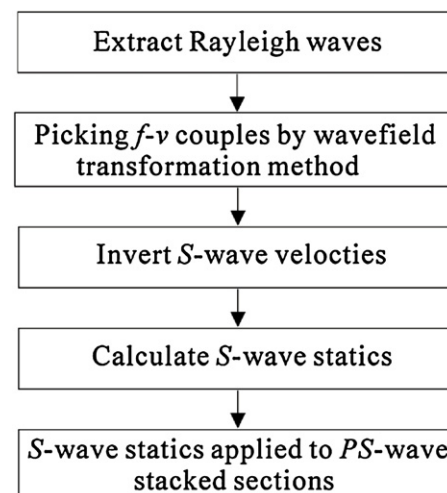


**Figure 2.** Process workflow of PS-wave static corrections.

However, there are many differences between PS- and P-wave exploration. For example, (a) the base of water table is not always an S-wave velocity interface since S-waves do not propagate in fluid (Deng *et al* 2004); (b) S-wave velocities present important lateral variations and it is difficult to choose a flat seismic datum; therefore, the determination of the datum is vitally important for PS-wave statics corrections.

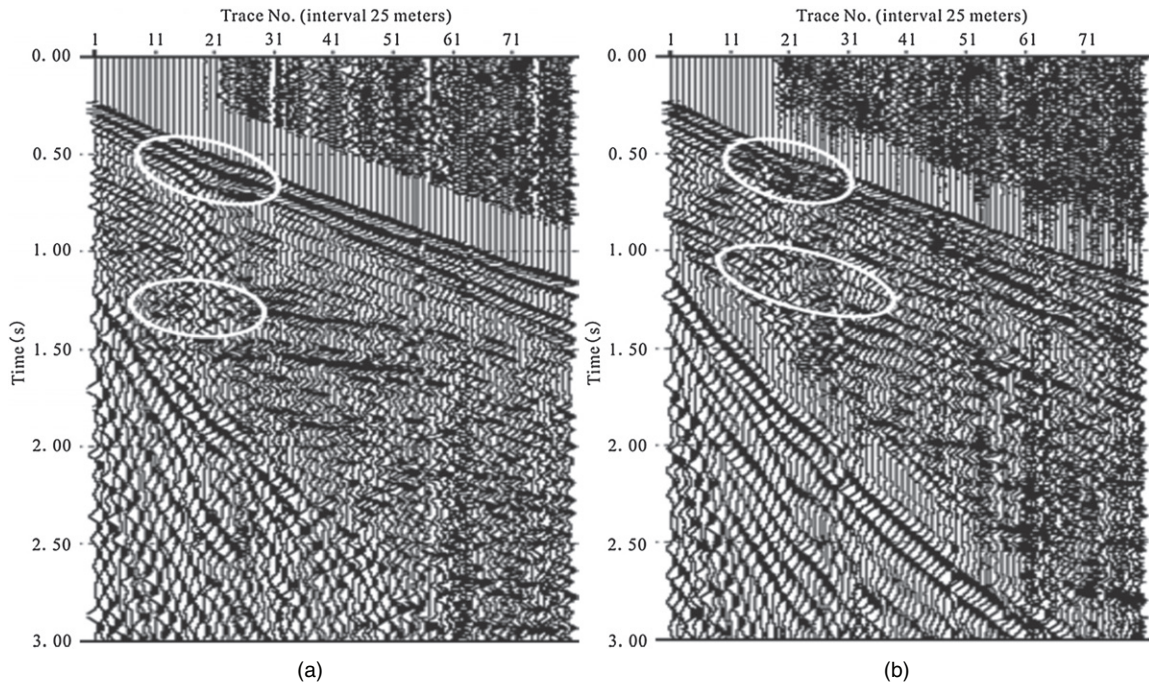


**Figure 3.** Shot records of multi-component in line S001, Daqing Oilfield, China, with (a) Z-component and (b) X-component.

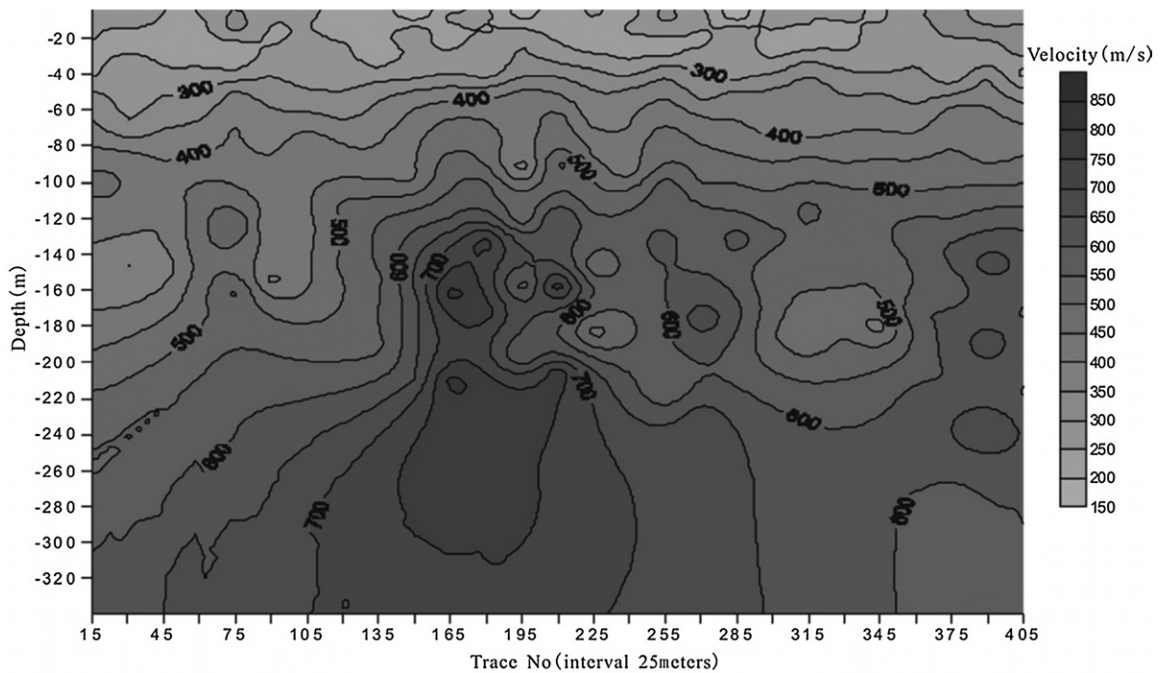


**Figure 4.** Inverted shear velocity model of line S001 in the Daqing Oilfield, China.

### 3. Application example

#### 3.1. A two-dimensional three-component case study

Two lines of 2D three-component seismic field data were acquired in Daqing Oilfield, China, in 1995, to improve the imaging of igneous rock reservoirs. Figure 3 shows the Z- and X-components of one shot in the line S001. Even though the surface is flat and the biggest difference in relief is only

a few metres in this area, the first arrivals and reflections in figure 3 show strong event distortions (denoted as the circles). Therefore, the statics of PS-waves should not be ignored. The S-wave velocity near-surface model, inverted by Rayleigh wave dispersion curves, is used to calculate PS-wave statics.

After extracting Rayleigh waves from Z-component records, S-wave velocities were predicted according to the method introduced in section 2, as shown in figure 4. This

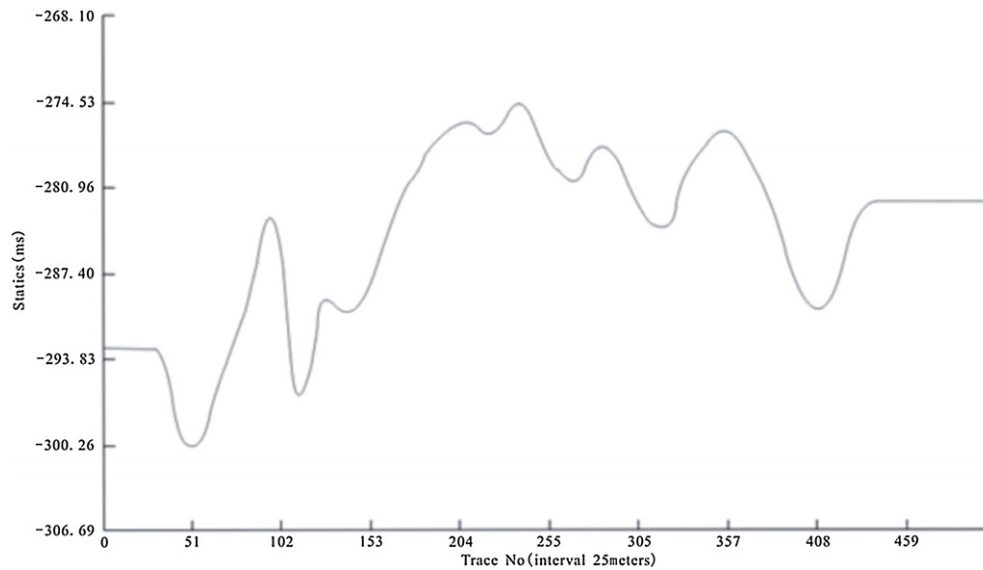


Figure 5. S-wave statics of receivers of line S001.

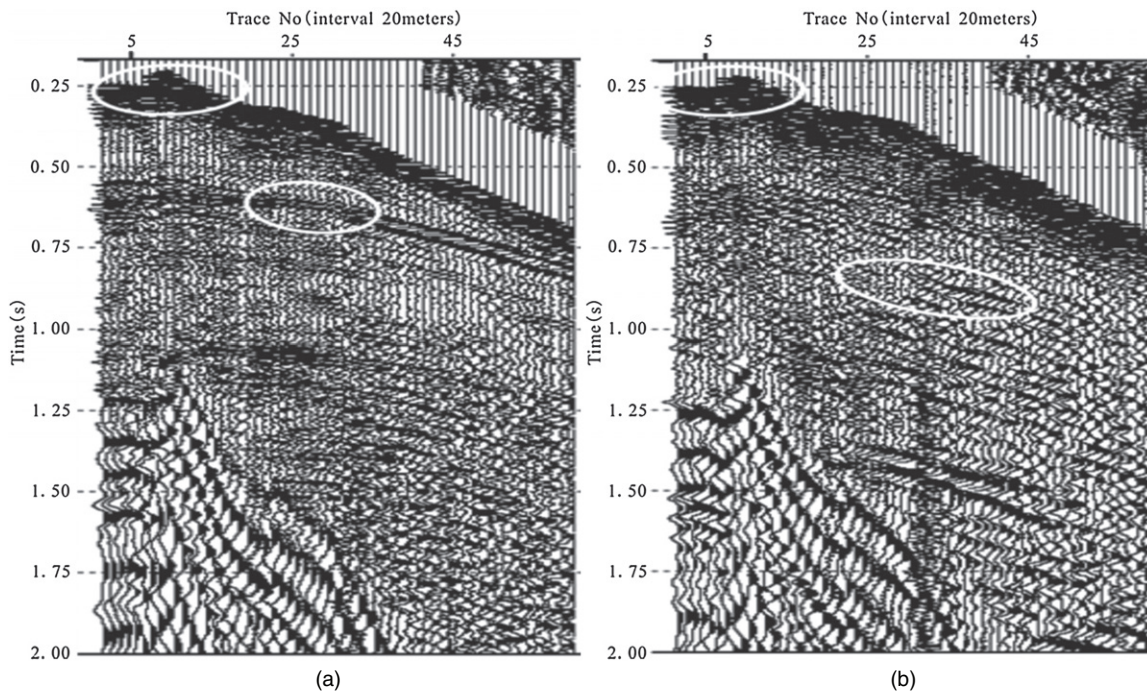


Figure 6. Two-component field records in the Huainan coal mine, with (a) Z-component and (b) R-component.

figure shows a very low S-wave velocity profile. At a depth of 20 m from the surface, the average S-wave velocities range from  $120 \text{ m s}^{-1}$  to  $200 \text{ m s}^{-1}$ . The discontinuity of S-wave velocities in the horizontal direction indicates that the frozen grounds near the surface or the Quaternary formations vary dramatically.

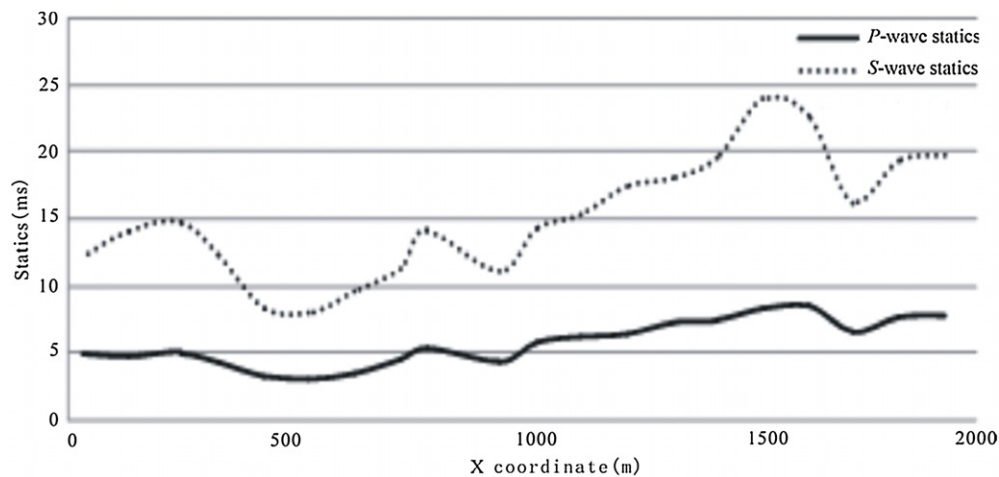
The base of the weathered layer is generally used as the seismic datum to compute P-wave statics in P-wave seismic explorations on land. The depth of the water table is almost the same as the depth of the weathered layer for P-waves. So, the water table, under which P-wave velocities are relatively large and stable, is usually used as the reference datum to

calculate P- and PS-wave statics (Cox 1999, Edge and Laby 1931).

In this case, the interpreted P-wave velocities indicate that the water table is only 2–3 m below the surface. Since there are no visible interfaces for S-waves at the water table in figure 4, the water table cannot be chosen as the seismic datum. According to the inversion results, the depth of the top boundary of the high velocity layer is 110 m for P-waves, and S-wave velocities are also high below this depth. So, we choose it as the datum for P- and PS- wave static corrections. After we establish the near-surface model, PS-wave statics are calculated integrated with P-wave statics. Figure 5 shows the

**Table 1.** S-wave statics at different receivers of Inline 157.

Source no.	X co-ordinates	Y co-ordinates	Shear velocity (m s <sup>-1</sup> )	Compressed velocity (m s <sup>-1</sup> )	P-wave statics (ms)	P- to S-wave velocity ratio	PS-wave statics (ms)
60 004	1930	1570	240.32	600.22	7.88	2.4976	19.68
60 012	1830	1570	241.95	600.12	7.79	2.4803	19.32
60 021	1730	1570	245.45	599.98	6.65	2.4444	16.26
60 030	1630	1570	226.21	599.85	8.59	2.6518	22.78
60 033	1530	1570	208.56	599.9	8.31	2.8764	23.90
60 046	1430	1570	230.87	600	7.51	2.5989	19.52
60 049	1330	1570	246.15	600.03	7.4	2.4376	18.04
60 063	1230	1570	221.68	600.01	6.46	2.7067	17.48
60 073	1130	1570	245.00	600.01	6.23	2.4490	15.26
60 076	1030	1570	243.47	599.99	5.83	2.4644	14.37
60 091	950	1570	236.09	599.98	4.42	2.5413	11.23
60 099	790	1570	227.52	600.03	5.38	2.6373	14.19
60 101	730	1570	240.55	600.05	4.59	2.4945	11.45
60 113	630	1570	215.06	600.17	3.48	2.7907	9.71
60 115	530	1570	227.05	600.49	3.06	2.6447	8.09
60 129	430	1570	243.51	600.08	3.43	2.4643	8.45
60 134	330	1570	211.24	599.48	4.38	2.8379	12.43
60 144	250	1570	208.51	599.75	5.13	2.8763	14.76
60 151	130	1570	200.50	599.97	4.73	2.9924	14.15
60 154	30	1570	254.64	599.84	5.14	2.3557	12.11

**Figure 7.** Statics of P- and PS-waves in Inline157.

PS-wave statics for the line S001. The average of PS-wave statics is 280 ms and the differences in S-wave time shifts at different receivers are high up to 26 ms. These indicate the presence of a serious horizontal heterogeneity for S-wave velocities.

### 3.2. A three-dimensional three-component case study

In seismic exploration used in coal mines, the precision of faults prediction should be high. In Huainan Coal Mine, southeastern China, we acquired a 3D three-component seismic data in 2003. Figure 6 shows a shot record of the field seismic data. The static time shifts are small in this area because the largest relief difference is only 2 m. However, static corrections are necessary if we want to identify minor faults. A similar processing flow is applied to invert S-wave velocity models for the three-dimensional seismic data.

However, it is difficult to find a datum for both P-wave and PS-wave static corrections in this case. To calculate PS-wave statics, we use S-wave velocities inverted from Rayleigh waves and P-wave velocities derived from P-wave reflections to calculate P- to S-wave velocity ratios. The solutions of multiplying P-wave statics by the P- to S-wave velocity ratios are considered as PS-wave statics. The statics, applied in PS-wave stack profiles, are shown in table 1. As illustrated in figure 7, PS-wave statics are two to four times larger than P-wave statics. However, the P- and S-wave statics have similar trends.

By comparing the PS-wave stack profiles in figure 8, it is clear that the events (around 1500–1700 ms) in the PS-wave stack profile, shown in figure 8(b), are improved comparatively to figure 8(a) after applying PS-wave static corrections. The PS-wave stack profile in figure 8(c) is further improved after applying residual static corrections to figure 8(b).

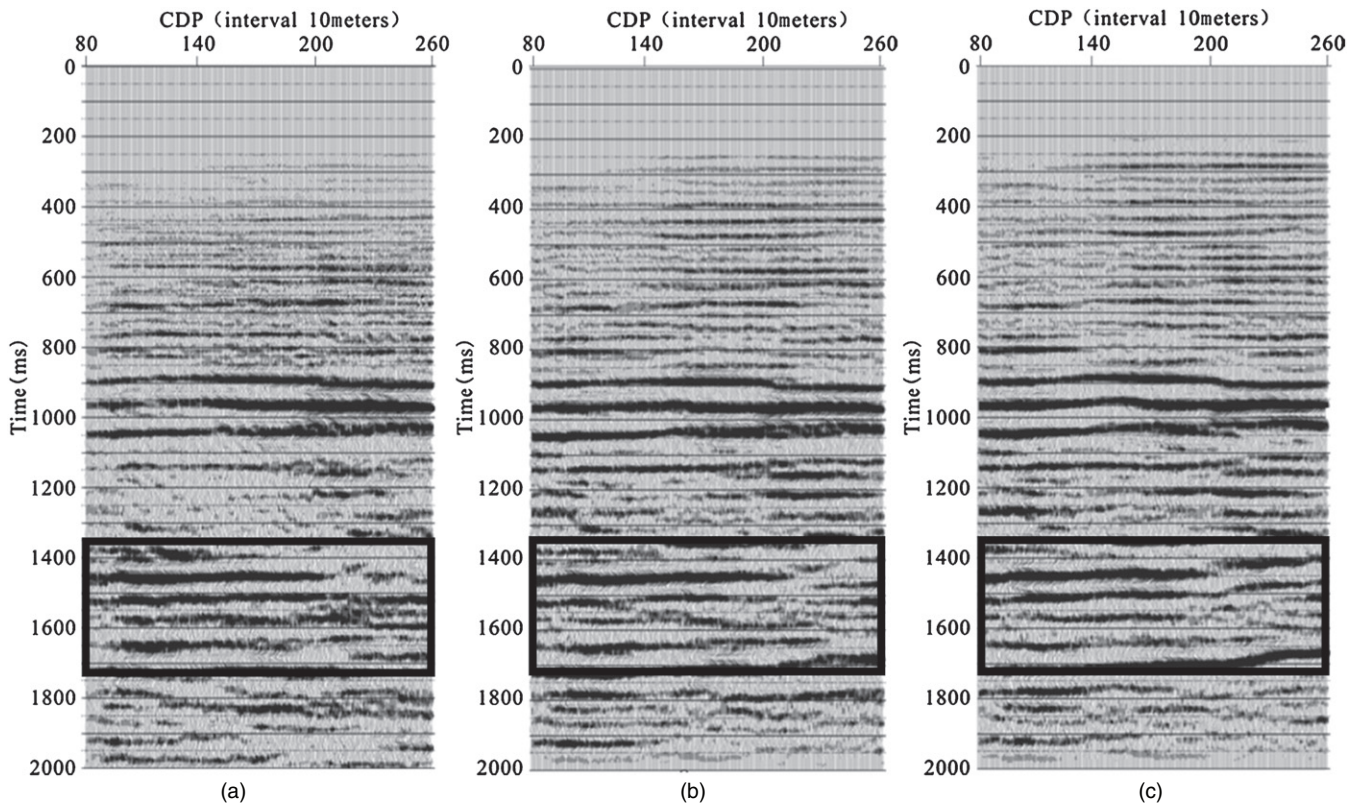


**Figure 8.** PS-wave stack profiles, in which (a) PS-wave stack profile without receiver static corrections, (b) PS-wave stack profile with receiver static corrections and (c) PS-wave stack profile with PS-wave static and residual static corrections.

#### 4. Conclusions

Due to lower S-wave velocity and horizontal discontinuity, receiver statics for PS-wave are often larger than those for P-waves. S-wave velocities are necessary for static corrections though they are difficult to obtain from the reflection data. To solve this problem without the acquisition of additional field data, Rayleigh waves can be employed to investigate the near-surface S-wave velocity structure and to calculate S-wave static corrections. In this paper, we have shown that the method is feasible and valuable in PS-wave static corrections and can be applied to process three-component seismic data.

#### Acknowledgments

The research is supported by China Natural Science Foundation (no 40574055) and National Special Fund (no 2011ZX05035-001-006HZ, 2011ZX05035-002-003HZ, 2011ZX05008-006-022, 2011ZX05049-01-02). The authors also thank Dr Yu for providing technical support to preprocess PS-wave data. We thank the referees for giving us constructive suggestions, which were valuable and very helpful in improving the manuscript.

#### References

Benhama A, Cllet C and Dubesset M 1988 Study and application of spatial directional filtering in three-component recordings *Geophys. Prospect.* **36** 591–613

- Cary P W and Eaton D W S 1993 A simple method for resolving large converted-wave (*P-SV*) statics *Geophysics* **58** 429–33
- Chang X, Liu Y, Wang H, Li F and Chen J 2002 3D tomographic static correction *Geophysics* **67** 1275–85
- Cox M 1999 *Static Corrections for Seismic Reflection Surveys* (Tulsa, OK: Society of Exploration Geophysicists)
- Deng Z W, Zou X F, Cui S T, Zhan S F, Zhao B L, Jiang X S, Guo Y B, He Y and Ni Y D 2004 Converted wave seismic exploration and static correction *SEG Int. Exposition and 74th Annual Meeting (Denver, CO)* pp 2549–52
- Dix C H 1955 Seismic velocities from surface measurements *Geophysics* **20** 68–77
- Edge A B and Laby T H 1931 *The Principles and Practice of Geophysical Prospecting* (London: Cambridge University Press) pp 339–41
- Graff K F 1975 *Wave Motion in Elastic Solids* (Oxford: Oxford University Press) p 325
- Grant F S and West G F 1965 *Interpretation Theory in Applied Geophysics* (New York: McGraw-Hill)
- Hearn S and Meulenbroek A 2011 Ray-path concepts for converted-wave seismic refraction *Explor. Geophys.* **42** 139–46
- Houck C R, Joines J and Kay M 1995 A genetic algorithm for function optimization 1–14 *NCSU-IE Technical Report* 95(09)
- Kano N, Yokokura T and Yamaguchi K 2003 A P–S converted-wave survey with severe statics problems on a Quaternary plain *Explor. Geophys.* **34** 151–7
- Lawton D C 1989 Nine-component refraction statics survey *CREWS Research Report* 3 pp 27–38
- Li Z C, Boadu F K and Brown R J 1990 Computing shear-wave statics with the help of seismic tomography *CREWS Research Report* vol 6 pp 67–79
- Meulenbroek A and Hearn S 2011 Analysis of converted refractions for shear statics and near-surface characterization *Explor. Geophys.* **42** 147–54

- Normark E 1993 Residual statics estimation by stack power maximization in the frequency domain *Geophys. Prospect.* **41** 551–63
- Palmer D 1986 Refraction seismics *Handbook of Geophysical Exploration* vol 13 (London: Geophysical Press)
- Park C B, Xia J H and Miller R D 1998 Imaging dispersion curves of surface waves on multichannel record *Annu. Int. Meeting Society of Exploration Geophysicists* vol 17 pp 1377–80
- Potel C and de Belleval J F 1995 Surface waves in an anisotropic periodically multilayered medium: influence of the adsorption *J. Appl. Phys.* **77** 6152–61
- Ronen J and Claerbout J F 1985 Surface-consistent residual estimation by stack-power maximization *Geophysics* **50** 2759–67
- Schafer A W 1989 Determination of shear-wave statics using converted, refracted waves from a compressional source *CREWES Project Research Report* vol 1 pp 67–79
- Schafer A W 1991 The determination of converted-wave static using P refractions together with SV refractions *SEG Technical Program Expanded Abstracts* pp 51–66
- Schwab F and Knopoff L 1970 Surface-wave dispersion computations *Bull. Seism. Soc. Am.* **60** 321–44
- Sheriff R E 1991 *Encyclopedic Dictionary of Exploration Geophysics* 3rd edn (Tulsa, OK: Society of Exploration Geophysicists)
- Sheriff R E and Geldart L P 1982 *Exploration Seismology* vol 1 (Cambridge: Cambridge University Press)
- Sheriff R E and Geldart L P 1995 *Exploration Seismology* 2nd edn (Cambridge: Cambridge University Press) p 49
- Tatham R H, McCormack M D, Neitzel E B and Winterstein D F 1991 *Multi-Component Seismology in Petroleum Exploration* (Tulsa, OK: Society of Exploration Geophysicists)
- Vasudevan K, Wilson W G and Laidlow W G 1991 Simulated annealing statics computation using an order based energy function *Geophysics* **56** 1831–9
- Wang B, Cheng S W, Pann K and Deng H L 1997 Estimating large statics by a simplified stacking power approach using local optimization *SEG Expanded Abstracts* **16** 1066–9
- Wiest B and Edelman H A K 2006 Static corrections for shear wave sections *Geophys. Prospect.* **32** 1091–102
- Xia J H, Miller R D and Park C B 1999 Estimation of near-surface shear-wave velocity by inversion of Rayleigh waves *Geophysics* **64** 691–700
- Yang C L 1993 *Surface Wave Exploration* (Beijing: Geology Publishing House) (in Chinese)
- Yao Y 1991 Calculating initial residual static with PS' reflection *Petroleum Exploration of Carbonate Reservoirs Expanded Abstracts* pp 121–5
- Zhao D, Hasegawa A and Horiuchi S 1992 Tomographic imaging of P and S wave velocity structure beneath northeastern Japan *J. Geophys. Res.* **97** B13 19909–28